Contribution from the Department of Chemistry, College of the Holy Cross, Worcester, Massachusetts 01610, and Department of Chemistry and Biochemistry, Utah State University, Logan, Utah 84322-0300

Kinetic and Spectroscopic Studies of Transients Produced by Flash Photolysis of $M(CO)_3(PR_3)_2X_2$ (M = Mo, W; X = Cl, Br)

Richard S. Herrick,*[†] Melinda S. George,[†] Ronald R. Duff, Jr.,[†] Felicitée Henry D'Aulnois,[†] Ronald M. Jarret,[†] and John L. Hubbard[‡]

Received September 12, 1990

Flash photolysis studies on a series of arylphosphine, alkylphosphine, and mixed aryl-alkylphosphine derivatives of $M(CO)_3(PR_3)_2X_2$ (M = Mo, W; X = Cl, Br) establish that two independent transients are produced photochemically. Each transient decays back to the tricarbonyl on the millisecond timescale under a carbon monoxide atmosphere. Spectroscopic, kinetic, and stopped-flow experiments demonstrate that the slower decaying transient (calculated bimolecular rate constants range from 5.3×10^2 to 7.3×10^5 M^{-1} s^{-1}) is the CO-deficient complex, $M(CO)_2(S)(PR_3)_2X_2$, where S is a weakly coordinated solvent molecule. Free energy relationships are used to probe effects on the rate of CO addition. The molecular structure of $Mo(CO)_2(PEt_3)_2Br_2$ is reported: tetragonal space group $P4_32_12$ with unit cell dimensions $a = b = 9.066$ (2) Å, $c = 25.852$ (6) Å, $Z = 4$, observed data = 1001, $R = 4.99\%$, and $R_w = 6.65\%$. The nonsymmetric orientation of the phosphine ethyl groups confirms that the cone angle for PEt_3 is 137° for these compounds. The fast-decaying transient (calculated bimolecular rate constants range from 1.4×10^5 to 1.0×10^6 M^{-1} s^{-1}) is observed for triarylphosphine derivatives with X = Br. Kinetic and product analysis experiments demonstrate that the transient is the phosphine-deficient complex $Mo(CO)_3(PR_3)(S)Br_2$. The transient is observed to rapidly combine with excess carbon monoxide before reacting with liberated phosphine to regenerate the starting tricarbonyl. The natural log of the rate constants fit a two-parameter free energy relationship based on the electronic nature of the phosphine and the effect of the metal. The bimolecular rate constants are compared to the rate constants for the reaction of the previously discovered CO loss photoproduct with CO.

Introduction

The class of compounds $M(CO)_n(PR_3)_2X_2$ (M = Mo, W; n = 2, 3; R = alkyl, aryl; X = Cl, Br) comprises a mononuclear group 6 system containing stable 16- and 18-electron members that co-exist in solution in chemical equilibrium.[1] The stability of the 16-electron dicarbonyl in the absence of carbon monoxide is especially interesting given the high reactivity and transient nature of 16-electron compounds such as $Cr(CO)_5$.[2] It is known that this stability stems from the 6-coordinate dicarbonyl, assuming a highly distorted geometry of nearly C_{2v} symmetry (Scheme I).[3] With the Cartesian orientation used by Hoffmann, this places the empty xz orbital above the filled yz and $x^2 - y^2$ orbitals. The four d electrons are paired and a large HOMO-LUMO gap results.

Previously, we showed that broadband irradiation of $Mo(CO)_3(PR_3)_2Br_2$ disrupts the equilibrium between the 16- and 18-electron species in solution by photoinducing CO dissociation.[4] Rapid chemical relaxation (with calculated bimolecular rate constants ranging from 2.5×10^3 to 7.3×10^5 M^{-1} s^{-1}) was observed despite the isolability of the dicarbonyl. Analysis of several phosphine derivatives demonstrated that large basic phosphine ligands inhibited CO recombination. Medium effects on the reaction rate and on the electronic spectrum showed that electron pairs from the solvent or solid medium interact with the LUMO of the dicarbonyl. In this sense, the localized interaction with the solvent is a weak-bonding interaction such that, in 1,2-dichloroethane (DCE) solution, the formula of the dicarbonyl may be written as $Mo(CO)_2(DCE)(PR_3)_2Br_2$. This localized interaction of solvent with a vacant coordination site is widely observed and the weakly ligated solvent molecule has been termed a "token ligand".[5]

We extended this research to include chloride and tungsten derivatives in order to analyze ligand and metal effects on the rate and made a number of unexpected findings. In this paper we report (1) the rate constants for CO addition to $M(CO)_2(DCE)(PR_3)_2X_2$ for all derivatives studied thus far, (2) apparent mechanistic differences for CO addition that depend on phosphine steric bulk, (3) a second photoproduct caused by phosphine loss from the starting tricarbonyl, (4) the molecular structure of $Mo(CO)_2(PEt_3)_2Br_2$, (5) rate constants for the reaction of the phosphine deficient transient with CO, and (6) linear free energy studies of ligand and metal effects on the rate for both reactions studied.

Scheme I

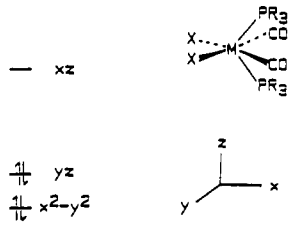

Experimental Section

Materials. Starting materials for syntheses were obtained commercially and used without further purification. Teflon was obtained as Chromosorb T 40/60 mesh from Supelco, Inc. Reagent grade $BaSO_4$ and spectroscopic grade KBr were employed. Carbon monoxide (99.97%) was purchased from Linde. 1,2-Dichloroethane was purified for flash photolysis by consecutive treatment with H_2SO_4/H_2O/saturated aqueous $NaHCO_3/H_2O/MgSO_4$ before distillation from P_2O_5. The same purification procedure was utilized for hexane prior to distillation from CaH_2. Benzene was washed with H_2SO_4 and distilled. Methanol was dried over molecular sieves and distilled from CaH_2.

Preparations. $M(CO)_3(PR_3)_2X_2$ (M = Mo, W; X = Cl, Br[1,4]) derivatives were prepared as described previously. Compounds were recrystallized at least two times from CH_2Cl_2/hexane prior to use. $W(CO)_2(PR_3)_2X_2$ (PR_3 = $P(C_6H_4$-p-$OMe)_3$, $P(C_6H_4$-p-$Me)_3$, PPh_3, $P(C_6H_4$-p-$F)_3$, PEt_3) was produced quantitatively by the literature method as a blue or purple solid.[3b] It typically took 1-3 days of reflux in CH_2Cl_2 to effect the change.

Spectroscopic Measurements. Infrared spectra were run on a Perkin-Elmer 1750 FT-IR spectrometer. Electronic spectra were recorded on a Perkin-Elmer Lambda 4C spectrometer. Diffuse reflectance spectra

[†] College of the Holy Cross.
[‡] Utah State University.

(1) (a) Colton, R.; Tomkins, I. B. *Aust. J. Chem.* **1966**, *19*, 1143. (b) Colton, R.; Tomkins, I. B. *Aust. J. Chem.* **1966**, *19*, 1519. (c) Anker, M. W.; Colton, R.; Tomkins, I. B. *Aust. J. Chem.* **1967**, *20*, 9. (d) Colton, R.; Scollary, G. R.; Tomkins, I. B. *Aust. J. Chem.* **1968**, *21*, 15.
(2) (a) Perutz, R. N.; Turner, J. J. *J. Am. Chem. Soc.* **1975**, *97*, 4791. (b) Bonneau, R.; Kelly, J. M. *J. Am. Chem. Soc.* **1980**, *102*, 1220. (c) Kelly, J. M.; Long, C.; Bonneau, R. *J. Phys. Chem.* **1983**, *87*, 3344. (d) Church, S. P.; Grevels, F.-W.; Hermann, H.; Schaffner, K. *Inorg. Chem.* **1984**, *23*, 3830.
(3) (a) Kubacek, P.; Hoffmann, R. *J. Am. Chem. Soc.* **1981**, *103*, 4320. (b) Cotton, F. A.; Meadows, J. H. *Inorg. Chem.* **1984**, *23*, 4688.
(4) Herrick, R. S.; Peters, C. H.; Duff, R. R. *Inorg. Chem.* **1988**, *27*, 2214.
(5) The term "token ligand" refers to a weakly interacting ligand, usually a solvent molecule, which occupies a specific coordination site of an organometallic intermediate following ligand loss. See: Dobson, G. R.; Hodges, P. M.; Healy, M. A.; Poliakoff, M.; Turner, J. J.; Firth, S.; Asali, K. J. *J. Am. Chem. Soc.* **1987**, *109*, 4218.

0020-1669/91/1330-3711$02.50/0

Table I. Crystallographic Data for $Mo(CO)_2(PEt_3)_2Br_2$

formula	$C_{14}H_{30}O_2P_2Br_2Mo$
mol wt	548.1
space group	$P4_32_12$
cryst syst	tetragonal
unit cell dimens	
a/Å	9.066 (2)
b/Å	9.066 (2)
c/Å	25.852 (6)
vol/Å^3	2125 (1)
T/°C	25
Z	4
ρ_{calcd}/g cm^{-3}	1.713
λ (Mo Kα)/Å	0.71073
cryst size/mm	0.05 × 0.24 × 0.26
μ/mm^{-1}	4.479
collectn range	$0 \le h \le 10$
	$0 \le k \le 10$
	$0 \le l \le 29$
2θ range/deg	3–48
F(000)	1088
no. of data collected	1966
no. of unique data (R_{int} = 6.86%)	1938
no. of obsd data with $F_o > 6\sigma(F_o)$	1001
no. of variables	97
extinction cor	$\chi = -0.00001$ (9), where $F^* = F[1 + 0.002\chi F^2/(\sin 2\theta)]^{-1/4}$
final R	0.0499
R_w	0.0665
weighting scheme, w	$[\sigma = 2(F) + 0.0013F^2]^{-1}$
data to param ratio	10.3:1
largest difference peak/e Å^{-3}	0.74
largest difference hole/e Å^{-3}	−0.73
abs cor	semiempirical (ψ scan)
transm coeff	1.000 (max)/0.6487 (min)

were obtained off the Lambda 4C instrument with a commercial reflectance sphere attachment. Spectra on $BaSO_4$ or KBr were obtained against a $BaSO_4$ reference. Spectra on Teflon were recorded against a Teflon background, since under experimental conditions Teflon was a better reflector. Spectra are plotted as the Kubelka-Munk equation[6] ($F(R_\infty) \equiv (1 - R_\infty)^2/2R_\infty = kc/s$, where $F(R_\infty)$ is the Kubelka-Munk function, R_∞ is the absolute reflectance of an infinitely thick sample, c is the molar concentration at high reflectance, s is the scattering coefficient, and k is the extinction coefficient) versus wavelength.

Fully coupled ^{13}C NMR spectra of $M(CO)_2(PEt_3)_2Br_2$ were recorded in $CDCl_3$ at −50 °C with a Bruker AC-300 spectrometer. A 45° tip angle was applied with a total recycle time between pulses of 10 s to ensure accurate carbonyl integrations. A digital resolution of 1.795 Hz/point was used along with an appropriate number of scans to achieve a signal to noise ratio of at least 8:1. Each spectrum showed a 1:2 relative intensity ratio of the downield carbonyl carbon to the upfield carbonyl carbon.

$Mo(CO)_3(PEt_3)_2Br_2$. ^{13}C NMR ($CDCl_3$): 246.1 (dd, $^2J_{C-P}$ = 44 Hz, $^2J_{C-P}$ = 9 Hz, capping CO), 222.5 (dd, $^2J_{C-P}$ = 25 Hz, $2J_{C-P}$ = 7 Hz CO).

$Mo(CO)_3(PEt_3)_2Cl_2$. ^{13}C NMR ($CDCl_3$): 250.1 (dd, $^2J_{C-P}$ = 44 Hz, $^2J_{C-P}$ = 10 Hz, capping CO), 225.7 (dd, $^2J_{C-P}$ = 26 Hz, $^2J_{C-P}$ = 7 Hz, CO).

$W(CO)_3(PEt_3)_2Br_2$. ^{13}C NMR ($CDCl_3$): 239.1 (dd, $^2J_{C-P}$ = 31 Hz, $^2J_{C-P}$ = 9 Hz, capping CO), 217.3 (dd, $^2J_{C-P}$ = Hz, 20 Hz, $^2J_{C-P}$ = 5 Hz, CO).

$W(CO)_3(PEt_3)_2Cl_2$. ^{13}C NMR ($CDCl_3$): 243.3 (dd, $^2J_{C-P}$ = 31 Hz, $^2J_{C-P}$ = 9 Hz, capping CO), 220.4 (dd, $^2J_{C-P}$ = 18 Hz, $^2J_{C-P}$ = 6 Hz, CO). ^{13}C NMR spectra of $Mo(CO)_2(PEt_3)_2Br_2$ and $W(CO)_2(PEt_3)_2Br_2$ in CH_2Cl_2 were obtained at −75 °C to look for bound CH_2Cl_2. No evidence was observed for bound CH_2Cl_2.

A summary of the key crystallographic data and parameters for structural determination of $Mo(CO)_2(PEt_3)_2Br_2$ are collected in Table I. Crystals of $Mo(CO)_2(PEt_3)_2Br_2$ were grown by layering hexane over a solution of methylene chloride containing the compound. A blue plate (0.5 × 0.24 × 0.26 mm) was mounted vertically on a glass fiber with epoxy cement and centered on a Nicolet R3m/V single-crystal diffractometer operating with graphite-monochromated Mo Kα radiation (λ = 0.71073 Å). The centering of 20 reflections $30° \le 2\theta \le 10°$ indicated a primitive tetragonal cell. The systematic absences pointed to the space group $P4_12_12$ or $P4_32_12$. Indeed, the structure could be solved and refined with equal success in either space group. An umambiguous choice between the enantiomeric space groups $P4_12_12$ and $P4_32_12$ could not be made on the basis of refining a free variable (η) based on the values of the imaginary components of the atomic scattering factors ($\Delta f''$). The free variable η refined to a value of −0.14 (7) in $P4_12_12$ and 0.14 (7) in $P4_32_12$. The structure was solved by direct methods (SHELTXTL PLUS).[7] Non-hydrogen atoms were located by using alternating cycles of least-squares full-matrix refinement followed by difference Fourier synthesis. Atomic scattering factors were used from the SHELTXTL-PLUS package of programs. Hydrogen atoms were generated in idealized positions and given fixed (0.06) isotropic thermal parameters. The data showed a convergence of R = 0.0499 and R_w = 0.0665. Non-hydrogen atoms were refined anisotropically. Bond lengths (Table II) and bond angles (Table III) are also provided.

Table II. Bond Lengths (Å) for $Mo(CO)_2(PEt_3)_2Br_2$

Mo(1)–Br(1)	2.600 (2)	Mo(1)–C(1)	1.96 (2)
Mo(1)–P(1)	2.459 (4)	Mo(1)–Br(1A)	2.600 (2)
Mo(1)–C(1A)	1.96 (2)	Mo(1)–P(1A)	2.459 (4)
C(1)–O(1)	1.15 (2)	P(1)–C(2)	1.85 (2)
P(1)–C(4)	1.81 (2)	P(1)–C(6)	1.80 (2)
C(2)–C(3)	1.50 (3)	C(4)–C(5)	1.50 (3)
C(6)–C(7)	1.52 (2)		

Table III. Bond Angles (deg) for $Mo(CO)_2(PEt_3)_2Br_2$

Br(1)–Mo(1)–C(1)	86.8 (5)	Br(1)–Mo(1)–P(1)	92.7 (1)
C(1)–Mo(1)–P(1)	89.6 (1)	Br(1)–Mo(1)–Br(1A)	89.6 (1)
C(1)–Mo(1)–Br(1A)	164.9 (5)	P(1)–Mo(1)–Br(1A)	117.6 (1)
Br(1)–Mo(1)–C(1A)	164.9 (5)	C(1)–Mo(1)–C(1A)	102 (1)
P(1)–Mo(1)–C(1A)	78.1 (4)	Br(1A)–Mo(1)–C(1A)	86.8 (5)
Br(1)–Mo(1)–P(1A)	117.6 (1)	C(1)–Mo(1)–P(1A)	78.1 (4)
P(1)–Mo(1)–P(1A)	138.8 (2)	Br(1A)–Mo(1)–P(1A)	92.7 (1)
C(1A)–Mo(1)–P(1A)	76.5 (5)	Mo(1)–C(1)–O(1)	178 (2)
Mo(1)–P(1)–C(2)	104.0 (5)	Mo(1)–P(1)–C(4)	121.0 (6)
C(2)–P(1)–C(4)	106.6 (9)	Mo(1)–P(1)–C(6)	115.9 (6)
C(2)–P(1)–C(6)	103.7 (7)	C(4)–P(1)–C(6)	104.1 (8)
P(1)–C(2)–C(3)	117 (1)	P(1)–C(4)–C(5)	114 (1)
P(1)–C(6)–C(7)	116 (1)		

Kinetics Studies. The apparatuses, experimental procedure, and data analysis for flash photolysis stopped flow measurements have been described elsewhere.[4]

Phosphine Scrambling Experiments. In a typical experiment, $W(CO)_3(PEt_3)_2Br_2$ (0.0146 g, 2.20 × 10^{-5} mol) and $Mo(CO)_2(PPh_3)_2Br_2$ (0.0184 g, 2.20 × 10^{-5} mol) were placed in a 100-mL Schlenk flask wrapped with aluminum foil. Following addition of 20 mL of distilled 1,2-dichloroethane and a 5-min CO sparge, a yellow homogeneous solution of the two tricarbonyls was obtained. A portion of the solution was syringed into an oxygen-free IR cell. A preliminary IR spectrum was recorded on a Perkin-Elmer 1750 FT-IR. The cell was placed against a Sunpak 321 S camera flash accessory (pulse duration around 0.5 ms; color temperature of 5500 K) and wrapped with aluminum foil. Spectra were obtained after 1, 2, 5, 10, 30, 50, and 70 camera flashes. No spectral changes were observed after 70 camera flashes. At the end of the experiment an IR spectrum was obtained on a portion of the solution remaining in the Schlenk flask. The spectrum was identical with the original spectrum. Each compound was also flashed separately in CO saturated 1,2-dichloroethane. No changes occurred in the IR spectrum.

Phosphine Substitution by Pyridine. Two equivalents of pyridine were added to $Mo(CO)_3(PPh_3)_2Cl_2$ in CH_2Cl_2. The original spectrum containing bands at 2030, 1964, and 1922 cm^{-1} shows new bands growing in at 2048 and 1944 cm^{-1} and a broadening of the 1964-cm^{-1} peak. Addition of further pyridine causes the new bands to increase in intensity. Addition of a large excess of pyridine did not produce a clean spectrum. No attempt was made to isolate products from this reaction.

Results

Kinetic Studies. Flash photolysis of $M(CO)_3(PR_3)_2X_2$ (M = Mo, W; X = Cl, Br) compounds in 1,2-dichloroethane under 1 atm of CO at 22 °C generates transients that are completely formed at the end of the 100-μs flash pulse. Decay traces for all chloride and triethylphosphine derivatives or for mixed aryl–al-

(6) (a) Frei, R. W.; MacNeil, J. D. *Diffuse Reflectance Spectroscopy in Environmental Problem-Solving*; CRC: Cleveland, OH, 1973. (b) Kortium, G. *Reflectance Spectroscopy; Principles, Methods, Applications*; Springer-Verlag: New York, 1969. (c) Ditzler, M. A.; Allston, R. A.; Casey, T. J.; Spellman, N. T.; Willis, K. A. *Appl. Spectrosc.* **1983**, *37*, 269.

(7) Siemens Analytical X-Ray Instruments, Madison, WI.

Table IV. Bimolecular Rate Constants for the Slow Process Due to the Reaction of $M(CO)_2(DCE)(PR_3)_2X_2$ with CO in 1,2-Dichloroethane at 22 °C

no.	compound[a]	k,[b] M^{-1}	λ_{max},[c] nm	θ,[d] deg	χ[e]
1	$Mo(CO)_2(DCE)(PEt_2Ph)_2Br$	7.3×10^5[f]		136	9.3
2	$Mo(CO)_2(DCE)(PEt_3)_2Br_2$	2.4×10^5[f]	568 (485)[f]	137[g]	6.3
3	$Mo(CO)_2(DCE)(PEt_3)_2Cl_2$	3.6×10^5		137[g]	6.3
4	$Mo(CO)_2(DCE)(PEtPh_2)_2Br_2$	5.8×10^5[f]		140	11.3
5	$Mo(CO)_2(DCE)[P(C_6H_4\text{-}p\text{-}OMe)_3]_2Br_2$	2.5×10^3[f]	610 (610)[f]	145	10.5
6	$Mo(CO)_2(DCE)[P(C_6H_4\text{-}p\text{-}OMe)_3]_2Cl_2$	5.3×10^2	582	145	10.5
7	$Mo(CO)_2(DCE)[P(C_6H_4\text{-}p\text{-}Me)_3]_2Br_2$	2.7×10^3[f]	611[f]	145	11.5
8	$Mo(CO)_2(DCE)(PPh_3)_2Br_2$	9.2×10^3[f]	610[f]	145	13.25
9	$Mo(CO)_2(DCE)(PPh_3)_2Cl_2$	2.4×10^3		145	13.25
10	$Mo(CO)_2(DCE)[P(C_6H_4\text{-}p\text{-}F)_3]_2Br_2$	1.5×10^4[f]		145	15.7
11	$Mo(CO)_2(DCE)[P(C_6H_4\text{-}p\text{-}Cl)_3]_2Br_2$	2.2×10^4[f]		145	16.80
12	$Mo(CO)_2(DCE)[P(C_6H_4\text{-}p\text{-}Cl)_3]_2Cl_2$	4.4×10^3	560[f]	145	16.80
13	$W(CO)_2(DCE)(PEt_2Ph)_2Br_2$	6.8×10^5		136	9.3
14	$W(CO)_2(DCE)(PEt_3)_2Br_2$	1.2×10^5	526 (690)	137[g]	6.3
15	$W(CO)_2(DCE)(PEt_3)_2Cl_2$	2.9×10^5		137[g]	6.3
16	$W(CO)_2(DCE)(PEtPh_2)_2Br_2$	4.2×10^5		140	11.3
17	$W(CO)_2(DCE)[P(C_6H_4\text{-}p\text{-}OMe)_3]_2Br_2$	1.8×10^3	568 (980)	145	10.5
18	$W(CO)_2(DCE)[P(C_6H_4\text{-}p\text{-}OMe)_3]_2Cl_2$	1.0×10^3		145	10.5
19	$W(CO)_2(DCE)[P(C_6H_4\text{-}p\text{-}Me)_3]_2Br_2$	2.2×10^3	562 (1030)	145	11.5
20	$W(CO)_2(DCE)(PPh_3)_2]_2Br_2$	3.5×10^3	558 (660)	145	13.25
21	$W(CO)_2(DCE)(PPh_3)_2Cl_2$	2.2×10^3		145	13.25
22	$W(CO)_2(DCE)[P(C_6H_4\text{-}p\text{-}F)_3]_2Br_2$	4.6×10^3	550 (840)	145	15.7
23	$W(CO)_2(DCE)[P(C_6H_4\text{-}p\text{-}Cl)_3]_2Br_2$	5.2×10^3	536 (850)	145	16.80
24	$W(CO)_2(DCE)[P(C_6H_4\text{-}p\text{-}Cl)_3]_2Cl_2$	2.1×10^3		145	16.80

[a] The metal parameter, ϕ, is 1970.1 cm^{-1} for Mo and 1964.9 cm^{-1} for W.[17] The halide parameter, γ, is 3.16 for Cl and 2.96 for Br.[16] See text for details. [b] Rate constants are accurate to ±10%. [c] Measured in CH_2Cl_2 or 1,2-dichloroethane. Extinction coefficient in parentheses (M^{-1} cm^{-1}). [d] Reference 14. [e] Reference 12c and 15. [f] Reference 4. [g] Corrected cone angle from ref 19.

kylphosphine derivatives showed a smooth first-order decay back to the baseline. The triarylphosphine bromide derivatives show a more complex behavior. There is a rapid first-order decay, complete in less than 1 ms, to give final absorbances above the initial baseline consistent with the presence of a second absorbing species. Monitored on a slower time scale, this signal exhibits an exponential decay back to the original baseline in less than 0.5 s (see supplemental data for examples of decay traces).

The slow process had previously been shown to have a linear dependence on CO concentration for $Mo(CO)_3(PPh_3)_2Br_2$, indicating a rate law first order in both CO and the metal-containing transient.[4] A similar dependence was observed when $W(CO)_3(PEt_3)_2Br_2$ was photolyzed under varying concentrations of CO (supplemental data). Bimolecular rate constants for the dicarbonyl recombination with CO ranged from 5.3×10^2 to 7.3×10^5 M^{-1} s^{-1} (Table IV).

Stopped-flow experiments were performed on the reaction of CO and $W(CO)_2(DCE)[P(C_6H_4\text{-}p\text{-}OMe)_3]_2Br_2$ in 1,2-dichloroethane showed that the dicarbonyl disappears exponentially over time. Assuming a CO concentration of 3.0×10^{-3} M, a rate of $(1.5 \pm 0.5) \times 10^3$ M^{-1} s^{-1} was obtained. This is within error limits of the value obtained by flash photolysis.

Flash photolysis experiments were also performed in different solvents to examine the recombination of the transient formed by photolysis of $W(CO)_3(PEt_3)_2Br_2$ with CO. Rate constants in hexane (2.2×10^5 M^{-1} s^{-1}), 1,2-dichloroethane (1.2×10^5 M^{-1} s^{-1}), and benzene (9.6×10^4 M^{-1} s^{-1}) were measured. The reaction rate was essentially quenched in methanol. An upper limit of 10 M^{-1} s^{-1} for the rate constant was estimated.

A linear dependence of the observed rate constant on CO concentration was recorded for the fast process for $W(CO)_3(PPh_3)_2Br_2$, demonstrating the first-order dependence of the process on CO concentration (supplemental data). Bimolecular rate constants for the fast process varied between 1.4×10^5 M^{-1} s^{-1} and 1.1×10^6 M^{-1} s^{-1} for the 10 triarylphosphine derivatives studied (Table V). The tungsten derivatives displayed a larger absorbance change for the fast transient than for the slow transient. Conversely, the molybdenum derivatives always showed a larger absorbance change for the slow transient.

Spectroscopic Studies. The λ_{max} of $W(CO)_2(DCE)(PEt_3)_2Br_2$ in 1,2-dichloroethane was measured as 526 nm. The λ_{max} of the transient following flash photolysis of $W(CO)_3(PEt_3)_2Br_2$, obtained by measuring the zero time absorbance as a function of wavelength, is 525 ± 5 nm. The λ_{max} of other transients agreed with the λ_{max} of the corresponding dicarbonyl. Diffuse reflectance spectroscopy was used to observe medium effects on the visible absorbance band of $W(CO)_2(S)(PEt_3)_2Br_2$ (S = weakly coordinated solvent or ion). The λ_{max} was measured as 585 nm on KBr, 678 nm on $BaSO_4$ and 800 nm on Teflon (supplemental data).

Table V. Bimolecular Rate Constants for the Fast Process Due to the Reaction of $M(CO)_3(PR_3)(DCE)Br_2$ with CO in 1,2-Dichloroethane at 22 °C

	phosphine complex	k,[a] M^{-1} s^{-1}	χ[b]	ϕ,[c] cm^{-1}
a	$Mo(CO)_3[P(C_6H_4\text{-}p\text{-}OMe)_3](DCE)Br_2$	*d*	10.5	1970.1
b	$W(CO)_3[P(C_6H_4\text{-}p\text{-}OMe)_3](DCE)Br_2$	1.0×10^6	10.5	1964.9
c	$Mo(CO)_3[P(C_6H_4\text{-}p\text{-}Me)_3](DCE)Br_2$	1.1×10^6	11.5	1970.1
d	$W(CO)_3[P(C_6H_4\text{-}p\text{-}Me)_3](DCE)Br_2$	6.0×10^5	11.5	1964.9
e	$Mo(CO)_3(PPh_3)(DCE)Br_2$	8.6×10^5	13.2	1970.1
f	$W(CO)_3(PPh_3)(DCE)Br_2$	3.3×10^5	13.2	1964.9
g	$Mo(CO)_3[P(C_6H_4\text{-}p\text{-}F)_3](DCE)Br_2$	3.9×10^5	15.7	1970.1
h	$W(CO)_3[P(C_6H_4\text{-}p\text{-}F)_3](DCE)Br_2$	2.2×10^5	15.7	1964.9
i	$Mo(CO)_3[P(C_6H_4\text{-}p\text{-}Cl)_3](DCE)Br_2$	2.3×10^5	16.8	1970.1
j	$W(CO)_3[P(C_6H_4\text{-}p\text{-}Cl)_3](DCE)Br_2$	1.4×10^5	16.8	1964.9

[a] Rate constants accurate to ±10%. [b] From refs 12c and 15. [c] From ref 17. [d] A decay trace was observed but had too small an absorbance change to be analyzed.

The region where the fast-decaying transient absorbs most strongly is between 400 and 600 nm. The wavelength of maximum absorbance could not be determined, however, since $M(CO)_2(DCE)(PR_3)_2Br_2$ is formed in large concentrations in the photolysis experiment and shows variable absorbance over the same region as the fast decay. Furthermore, the concentration of the fast transient formed following the flash was not very reproducible. Under pseudo-first-order conditions, λ_{max} is determined by plotting absorbance versus optical density for a series of flashes. This only succeeds if the same concentration of transient is produced in each event.

Molecular Structure of $Mo(CO)_2(PEt_3)_2Br_2$. The solid-state molecular structure of $Mo(CO)_2(PEt_3)_2Br_2$ is shown in Figure 1. The Mo(1) atom lies on a 2-fold axis of the tetragonal cell. The geometry may be viewed as a highly distorted octahedron. The atoms Mo(1), C(1), C(1A), Br(1), and Br(1A) form a plane with deviations of ±0.28 Å. The P(1)–Mo(1)–P(1A) plane is 78.5° to the previous plane. The Br(1)–Mo–Br(1A) angle is 86.9° and the C(1)–Mo–C(1A) angle is 102.3°. Both phosphines are severely distorted away from the axial sites of an octahedron with

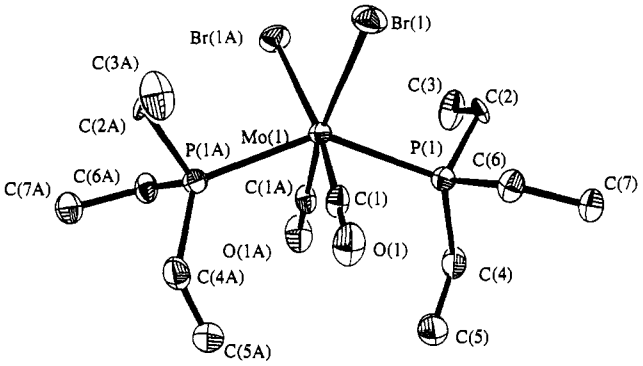

Figure 1. Molecular structure of $Mo(CO)_2(PEt_3)_2Br_2$ showing the atom-labeling scheme.

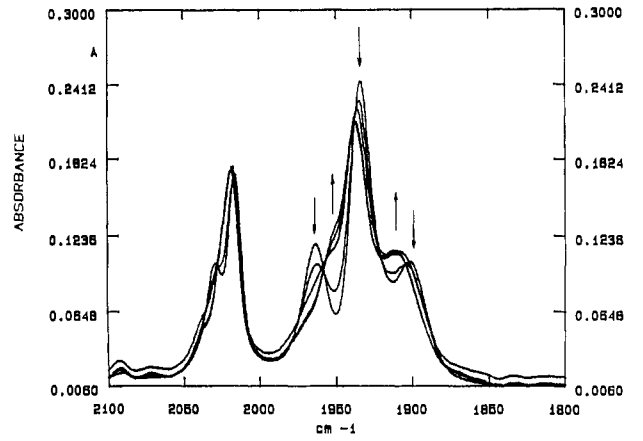

Figure 2. Infrared spectra following 0, 10, 30, 50, and 70 flash pulses from a millijoule flash photolysis source of a 1,2-dichloroethane solution equimolar in $Mo(CO)_3(PPh_3)_2Br_2$ and $W(CO)_3(PEt_3)_2Br_2$. Arrows signal the growth and disappearance of bands in the region between 1900 and 1970 cm^{-1}.

a P(1)–Mo–P(1A) angle of 138.8°. The ethyl groups of the triethyl phosphine are unsymmetrically oriented around the phosphorus atoms. In each phosphine one ethyl group is pointed away from the metal center while the other two ethyl groups are situated so that the pendant methyls are bent back slightly toward the metal. Bond distances within the molecule are unexceptional.

Phosphine Substitution Experiments. The infrared spectrum of a CO-saturated solution of $Mo(CO)_3(PPh_3)_2Br_2$ and $W(CO)_3(PPh_3)_2Br_2$ in 1,2-dichloroethane was monitored following millijoule flash pulses until no further change occurred (Figure 2). Before photolysis the spectrum showed bands at 1901 (m), 1934 (s), 1963 (m), 2016 (m), and 2028 (sh) cm^{-1}. After one flash, changes were apparent. After 70 flashes no further change was observed. The final spectrum showed bands at 1912 (m), 1937 (s), 1952 (sh), 2018 (m), and 2036 (w, sh) cm^{-1}.

Loss of phosphine could also be induced in the presence of pyridine. Addition of 2 equiv of pyridine to a CH_2Cl_2 solution of $Mo(CO)_3(PPh_3)_2Cl_2$ produces a spectrum consistent with a mixture of $Mo(CO)_3(PPh_3)_2Cl_2$ and $Mo(CO)_3(PPh_3)(py)Cl_2$. The starting tricarbonyl pattern at 2030, 1964, and 1922 cm^{-1} decreases in intensity and a new tricarbonyl pattern at 2048, 1978, and 1919 cm^{-1} is observed. The new tricarbonyl pattern is different than the patterns for $Mo(CO)_3(PPh_3)_2Cl_2$ and $Mo(CO)_3(py)_2Cl_2$.[8]

Discussion

Reaction of CO with $M(CO)_2(DCE)(PR_3)_2X_2$. The slow reaction observed for arylphosphine bromide derivatives and the only reaction observed for the remaining derivatives is ascribed to the reaction of the CO-deficient dicarbonyl with CO. This process was previously reported for the molybdenum bromide derivatives.[4] Similar evidence has been acquired to propose that this process is general for all metal and halide derivatives studied. The observed rate constant was measured at various CO concentrations for $W(CO)_3(PEt_3)_2Br_2$ demonstrating that the rate law was first order in CO as well as the transient, supporting the contention that the transient is reacting with CO. The transient was identified as the dicarbonyl because the electronic spectrum of $W(CO)_2(PEt_3)_2Br_2$ in CH_2Cl_2 agrees very closely with the transient spectrum, and rate constants from flash photolysis and stopped flow experiments obtained for $W(CO)_2[P(C_6H_4\text{-}p\text{-}OMe)_3]_2Br_2$ agree within experimental error.[9]

Electronic spectra of $W(CO)_2(PEt_3)_2Br_2$ in various media demonstrate that the solvent or solid substrate interacts with the LUMO of the dicarbonyl. The λ_{max} for the d–d band shifts 270 nm to lower energy upon changing from 1,2-dichloroethane to solid $BaSO_4$, to KBr and finally to Teflon as the substrate. This is more than the 190-nm shift observed in a similar study on $Mo(CO)_2(PEt_3)_2Br_2$.[4] Further evidence of a solvent effect is that the relatively good Lewis base methanol essentially quenches back reaction with carbon monoxide. Thus the dicarbonyl in solution is best formulated as the solvated complex, $M(CO)_2(S)(PR_3)_2X_2$, and the reaction with CO following flash photolysis becomes

$$M(CO)_2(S)(PR_3)_2Br_2 + CO \rightarrow M(CO)_3(PR_3)_2Br_2 + S \quad (1)$$

S = solvent

The electronic spectra demonstrate that the magnitude of the interaction of the substrate with the LUMO is in the order CH_2Cl_2 > KBr > $BaSO_4$ > Teflon. This is the order found for $Mo(CO)_2(PEt_3)_2Br_2$ and can be viewed as the ordering of substrate nucleophilicities toward the dicarbonyl. It has been previously observed that CH_2Cl_2 can occupy a vacant coordination site with one or both chlorides behaving as a Lewis base,[10] and halide adducts of related compounds have been isolated.[11] The sulfate ion should have less nucleophilic character than the halide while perfluoroalkanes are known to have little or no interaction with complexes with vacant coordination sites.[2a-c]

Complexes which achieve an 18-electron count through weak interactions with the solvent acting as a token ligand are increasingly common.[5] This series of compounds differs from other compounds previously studied, because they form stable, isolable 16-electron species in which the stability of the isolated compound is explained by the HOMO–LUMO gap afforded by the highly distorted nonoctahedral geometry. Formation of a solvated complex clearly does occur in solution, however, because the LUMO is still relatively low in energy.

While electronic spectra and flash photolysis in different solvents show that solvation occurs for the dicarbonyls, this interaction was not observed in the ^{13}C NMR spectrum of $M(CO)_2(CH_2Cl_2)(PEt_3)_2Br_2$ (M = Mo, W) at −75 °C nor was a solvent adduct observed in the crystal structure of $Mo(CO)_2(PEt_3)_2Br_2$ or $W(CO)_2(PPh_3)_2Br_2$.[3b] This implies that the solvent is more weakly bound than in some related complexes. For example, $[(C_5H_5)Re(NO)(PPh_3)_2(ClCH_2Cl)]^+$ was clearly observed by NMR at −85 °C,[10d] and $Ag_2(CH_2Cl_2)_4Pd(OTeF_5)_4$, in which four Cl atoms from two methylene chlorides are coordinated to each silver center, was studied by X-ray crystallography.[10a]

Free Energy Relationships for Reaction of the Dicarbonyl with CO. The bimolecular rate constants for all derivatives show the expected dependence on the phosphine. Electron-donating

(8) (a) $Mo(CO)_3(py)_2Br_2$ is an unstable compound prepared from addition of stoichiometric amounts of py to $Mo(CO)_4Br_2$. IR (CH_2Cl_2) shows strong carbonyl stretches at 2054, 1960, and 1942 cm^{-1}. On standing or with a slow nitrogen stream irreversible CO loss leads to the isolable $Mo(CO)_2(py)_2Br_2$. (b) Herrick, R. S. Unpublished observations. (c) Colton, R.; Rix, C. J. *Aust. J. Chem.* **1968**, *21*, 1155.

(9) Rate constants obtained by stopped flow had a higher uncertainty than those obtained by flash photolysis. This was attributed to slow leakage of CO from the system.

(10) (a) Newbound, T. D.; Colsman, M. R.; Miller, M. M.; Wulfsberg, G. P.; Anderson, O. P.; Strauss, S. H. *J. Am. Chem. Soc.* **1989**, *111*, 3762. (b) Beck, W.; Schloter, K. *Z. Naturforsch.* **1978**, *33B*, 1214. (c) Fernandez, J. M.; Gladysz, J. A. *Inorg. Chem.* **1986**, *25*, 2672. (d) Fernandez, J. M.; Gladysz, J. A. *Organometallics* **1989**, *8*, 207.

(11) (a) Burgmayer, S. J. N.; Templeton, J. L. *Inorg. Chem.* **1985**, *24*, 2224. (b) Herrick, R. S.; Templeton, J. L. *Inorg. Chem.* **1986**, *25*, 1270.

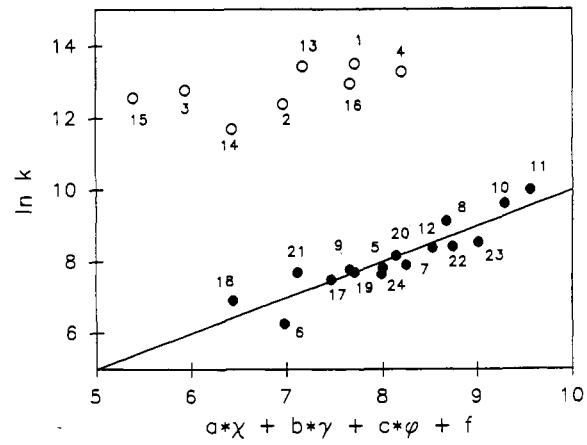

Figure 3. Linear relationship obtained by multiple linear regression for triaryl phosphine derivatives (filled circles) when plotted with the equation $\ln k_{expt} = a\chi + b\gamma + c\phi + f$. A correlation coefficient of 0.914 was obtained between the observed and calculated values of $\ln k_{expt}$. Other phosphine derivatives are plotted as hollow circles. Refer to Table IV for numbering system.

phosphines inhibit the rate (cf. the rates for $W(CO)_2(DCE)[P(C_6H_4\text{-}p\text{-}OMe)_3]_2Br_2$ and $W(CO)_2(DCE)[P(C_6H_4\text{-}p\text{-}Cl)_3]_2Br_2$), and sterically bulky phosphines also inhibit the rate (the rate constant for $W(CO)_2(DCE)(PEt_3)_2Br_2$ is nearly 2 orders of magnitude larger than the rate for $W(CO)_2(DCE)(PPh_3)_2Br_2$ despite the greater basicity of PEt_3). Tungsten derivatives were observed to have smaller rate constants than the corresponding molybdenum derivatives. The effect of the halides was not as clear-cut. For the triarylphosphine derivatives, the bromide compounds reacted more rapidly while for the PEt_3 derivatives the chloride compounds reacted more rapidly.

To quantitatively measure the effect of the phosphine, metal, and halide on the rate, free energy relationships were examined for these compounds, adapting methods of dealing with phosphine steric effects recently developed independently by Giering[12] and Poë.[13] This depends on splitting the rate constant into additive contributions of the steric and electronic factors. Analysis of ln k_{expt}, in which k_{expt} is the experimental bimolecular rate constant, at constant phosphine cone angle gives the isosteric plot.

We used this method with the addition of factors to account for the contributions of the metal and the halide to examine the free energy relationship for all derivatives studied. The free energy relationship in eq 2 was employed, where the electronic parameter

$$\ln k_{expt} = a\chi + b\gamma + c\phi + d\theta + e \qquad (2)$$

of the phosphine is given by χ,[12c,14,15] the Pauling electronegativity values[16] for chlorine and bromine are used as the halide parameter (γ), the t_{1u} ν(CO) stretch[17] of $Mo(CO)_6$ and $W(CO)_6$ is used as the metal parameter (ϕ), and the cone angle of the phosphine is given by θ.[14] Both γ and ν are empirical parameters, since it is not possible to separate electronic effects from steric effects for the metal or the halide.[18]

A multiple linear regression (Minitab, version 7.1, Minitab, Inc.) was performed on the 16 triarylphosphine derivatives that have $\theta = 145°$ to obtain the isosteric plot. Figure 3 shows the resulting plot of ln k_{expt} vs $a\chi + b\gamma + c\phi + f$ (where $d\theta + e$ have been combined into one constant). The values of the coefficients were $a = 0.214$, $b = -4.26$, $c = 0.128$, and $f = -234$. The sign of the phosphine electronic coefficient (a) indicates that increasing the electron-donating ability of the phosphine decreases the rate as expected. The signs of b and c indicate that tungsten as the metal and chloride as the halide inhibit the rate.

The steric contribution of the phosphine to the rate can now be obtained by rearranging eq 2 to the form

$$\ln k_{expt} - (a\chi + b\gamma + c\phi + e) = d\theta \qquad (3)$$

Giering and co-workers recently analyzed our previously published data for CO addition to $Mo(CO)_2(DCE)(PR_3)_2Br_2$ in this fashion to obtain a steric profile for these compounds.[12d] They obtained a plot that could be represented as two joined straight lines meeting at 139°. Calculations using all derivatives (unfortunately, only derivatives with four different cone angles could be prepared for this system) show that there is no steric effect on the rate for phosphines with cone angles smaller than 137°, and there is an increasingly large inhibitory effect on the rate of recombination for all larger phosphines measured. We estimate the steric threshold at which the phosphine begins to affect the rate to be 139°. This is the same value obtained by Giering et al. for the smaller set of $Mo(CO)_2(PR_3)_2Br_2$ compounds.[12d] Parenthetically, it should be pointed out that the cone angle used for PEt_3 is 137°, as suggested by Ernst et al.,[19] rather than the 132° value in Tolman's tables.[14] Use of the corrected value is clearly required here, because the phosphines in the crystal structure of $Mo(CO)_2(PEt_3)_2Br_2$ each have two pendant methyl groups bent back toward the metal (Figure 1). The original value of 132° for PEt_3 was obtained by assuming a symmetrical structure with all three ethyl groups folded away from the metal. Bound PEt_3 is more often found to have the geometry seen in $Mo(CO)_2(PEt_3)_2Br_2$.

A discontinuous effect of phosphine cone angles on the rate has previously been observed in several cases.[12] It was explained that for smaller phosphines ($\theta \leq 137°$ in this study) there is no steric effect on the rate due to the rate insensitivity to the incoming CO of derivatives with small phosphines. This occurs when the vacant hole created by the bound phosphines is larger than the incoming CO in both the ground and transition states. The increasingly larger inhibitory effect on the rate as the phosphine girth increase ($\theta \geq 145°$) indicates a region where the more sterically encumbered transition state is sensitive to the size of the phosphine. The rate decreases with increasing phosphine size as the CO must overcome increasing steric interactions in approaching the metal.[20]

One can now examine the free energy relationship $\ln k_{expt} = b'\gamma + c'\phi + f'$ for just the PEt_3 derivatives. This is the isosteric relationship for the PEt_3 derivatives. Since the electronic effect of the phosphine is constant it moves into the constant, f'. The expected linear relationship (with a correlation coefficient of 0.956) from multiple linear regression obtains with $b' = 0.082$, $c' = 3.212$, and $f' = -169$ (see supplemental data for figure). The important fact to notice is that b' is positive (with an 85% confidence level) while for the triarylphosphine derivatives b is negative (with a 99% confidence level). This is consistent with the observation that triethylphosphine dicarbonyl chloride derivatives react more rapidly than the corresponding bromide derivatives with CO. In contrast the triarylphosphine chloride dicarbonyl compounds react more slowly with CO than the corresponding bromides (cf. Table IV).

(12) (a) Golovin, M. N.; Rahman, Md. M.; Belmonte, J. E.; Giering, W. P. *Organometallics* **1985**, *4*, 1981. (b) Rahman, Md. M.; Liu, H.-Y.; Prock, A.; Giering, W. P. *Organometallics*, **1987**, *6*, 650. (c) Rahman, Md. M.; Liu, H.-Y.; Eriks, K.; Prock, A.; Giering, W. P. *Organometallics* **1989**, *8*, 1. (d) Eriks, L.; Giering, W. P.; Liu, H.-Y.; Prock, A. *Inorg. Chem.* **1989**, *28*, 1759.

(13) (a) Dahlinger, K.; Falcone, F.; Poë, A. J. *Inorg. Chem.* **1986**, *25*, 2654. (b) Poë, A. J. *Pure Appl. Chem.* **1988**, *60*, 1209. (c) Chen, L.; Poë, A. J. *Inorg. Chem.* **1989**, *28*, 3641.

(14) Tolman, C. A. *Chem. Rev.* **1977**, *77*, 313.

(15) Bartik, T.; Himmler, T.; Schulte, H.-G.; Seevogel, K. *J. Organomet. Chem.* **1984**, *272*, 29.

(16) Huheey, J. E. *Inorganic Chemistry*, 3rd ed.; Harper & Row: New York, 1983.

(17) Jones, L. H.; McDowell, R. S.; Goldblatt, M. *Inorg. Chem.* **1969**, *8*, 2349.

(18) It is assumed, however, that the steric effect of the metal is negligible, since molybdenum(II) and tungsten(II) radii are nearly identical.

(19) Stahl, L.; Ernst, R. D. *J. Am. Chem. Soc.* **1987**, *109*, 5673.

(20) Such a plot with two straight line portions was proposed by Giering et al. to be representative of the difference in free energies of the ground and transition states for an associative reaction. Below some cone angle called the steric threshold, there is no effect of the cone angle on the rate, because the hole made by the appropriate bound ligands for the incoming CO is larger than the CO. In contrast, Poë et al. believe that these plots should be presented with a smooth curve because the inherent uncertainty in the kinetic and steric factors and the effect of the cone angles will lead to pronounced deviations from a rigid two-line plot.

Scheme II

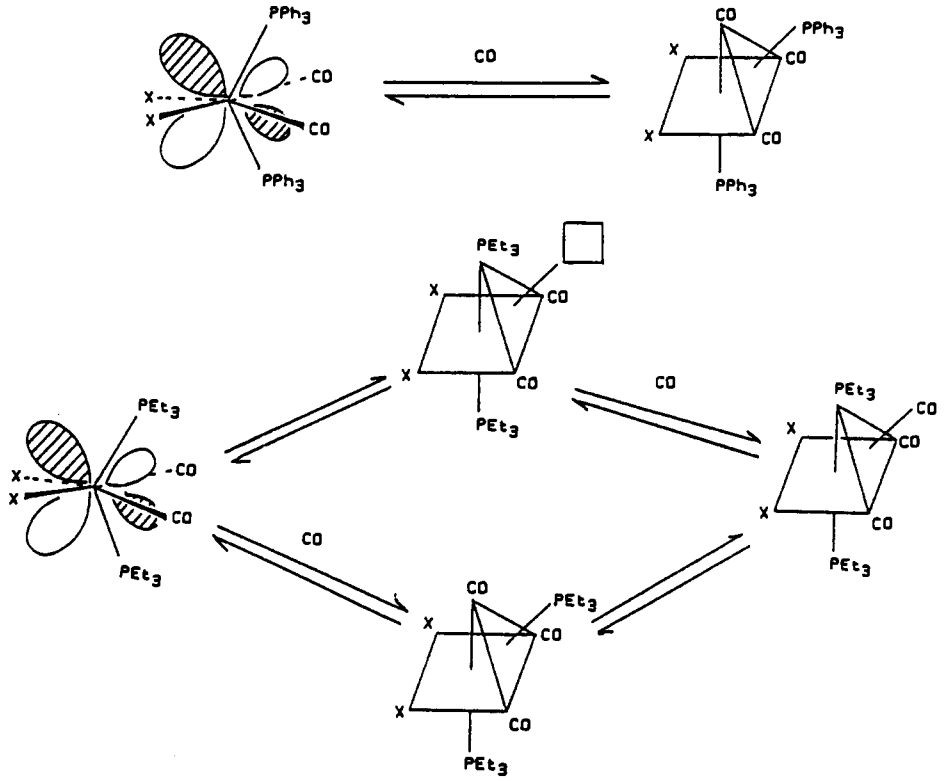

This strongly suggests that the details of the mechanism involved in the two cases are different.

Mechanistic Effect of Steric Bulk on CO Addition to $M(CO)_2(S)(PR_3)_2X_2$. Stopped-flow experiments, k_{obs} vs [CO] plots, and comparison of electronic spectra of photochemically generated transients against spectra of synthetically obtained dicarbonyls clearly show that $M(CO)_2(S)(PR_3)_2X_2$ is the spectroscopically observed transient and that it adds CO, but no further mechanistic details can be gleaned from these studies. Molecular structures of triethylphosphine and triarylphosphine derivatives of the ground-state dicarbonyl and tricarbonyl complexes have been compared to look for differences due to differing steric demands that might lead to mechanistic variations. The molecular structure of $Mo(CO)_2(PEt_3)_2Br_2$ was obtained to determine if it was different than the known structure of $W(CO)_2(PPh_3)_2Br_2$.[3b] The structures are quite similar in that each is a greatly distorted octahedron with formally trans phosphines and mutually cis pairs of carbonyls and bromides. In each compound, the phosphines are greatly distorted away from the vertical and lie over the bromides. The carbonyls are each separated by an angle greater than 90° (M = Mo, 102.3°; M = W, 110°), the bromides are separated by an angle of less than 90° (M = Mo, 86.9°; M = W, 82.0°), and the phosphines are separated by angles much less than 180° (M = Mo, 138.6°; M = W, 128.3°). Thus the molybdenum is consistently less distorted than the tungsten complex, though these differences alone do not constitute an explanation for the differing dependences of the rate constants on the identity of the halide.[21]

The solid-state structure of $Mo(CO)_3(PEt_3)_2Br_2$ is a capped octahedron with a carbon monoxide capping ligand.[22] Conversely, the solution structure of $Mo(CO)_3[P(C_6H_4\text{-}p\text{-}Me)_3]_2X_2$ (X = Cl, Br) has been shown to be a capped octahedron with a $P(C_6H_4\text{-}p\text{-}Me)_3$ capping ligand by ^{13}C NMR.[23] $Mo(CO)_3(AsPh_3)_2Cl_2$ and $Mo(CO)_3(SbPh_3)_2Br_2$, with sterically less demanding group 15 donor atoms, were each shown to adopt a capped octahedral configuration in solution with a CO capping the octahedron.[24] To confirm that the solution structure of the 7-coordinate PEt_3 complex mirrored the solid-state structure, ^{13}C NMR spectra of $M(CO)_3(PEt_3)_2X_2$ (M = Mo, W; X = Cl, Br) were obtained. The 1:2 relative intensities of the downfield carbonyl carbon to the upfield carbonyl carbon (the pattern observed for the $AsPh_3$ and $SbPh_3$ derivatives) verify that the solution structure of the PEt_3 derivatives is a capped octahedron with a carbon monoxide capping ligand. This substantiates the prediction Colton and Kevekordes made that compounds in this series with small group 15 donor ligands will prefer the CO capped octahedral structure.[23]

The significance of the tricarbonyl structural differences is apparent when one examines how CO is expected to attack in each case (Scheme II). For triarylphosphine derivatives, a one-step process would prevail. The LUMO (primarily *xz* in character) of the dicarbonyl, which has two lobes of high orbital probability extending above and below the two halides, is shown. The incoming CO can attach itself to either lobe, and minor reorganization leads directly to the ground-state structure of the tricarbonyl.

Simple attachment of the CO to the LUMO of the PEt_3 dicarbonyl derivative must be accompanied by rearrangement to obtain the ground-state structure of the tricarbonyl. Alternatively, the rearrangement can precede the CO attack. The process of CO attachment preceding rearrangement was observed previously for the conceptually similar reaction of Lewis base addition to the stable 16-electron complex, $Mo(CO)_2(S_2CNR_2)_2$.[25] Crystallographic studies of several adducts formed by ligands of varying basicity were used to demonstrate that ligand addition to the formally electron deficient compound occurs at the site where the LUMO orbital density is localized and is followed by molecular reorganization for more basic Lewis bases.

(21) (a) The angle between the two carbonyls in the dicarbonyls in solution as determined from the relative infrared carbonyl stretch intensities is between 112 and 120°, implying that the structures of all dicarbonyls in solution are similar. (b) Cotton, F. A.; Wilkinson, G. *Advanced Inorganic Chemistry*, 4th ed.; John Wiley and Sons, Inc.: New York, 1980.

(22) Drew, M. G. B.; Wilkins, J. D. *J. Chem. Soc., Dalton Trans.* **1977**, 194.

(23) Colton, R.; Kevekordes, J. *Aust. J. Chem.* **1982**, *35*, 895.

(24) The method compares the carbonyl peak intensities and chemical shifts of numerous Mo(II) heptacoordinate complexes and comparison with known structures to identify the solution geometries of many 7-coordinate molybdenum compounds.

(25) Templeton, J. L.; Burgmayer, S. J. N. *Organometallics* **1982**, *1*, 1007.

Reaction of $M(CO)_3(PC_6H_4$-*p*-$X)(DCE)X_2$ with CO. The fast-decaying transient was only observed for triarylphosphine bromide derivatives. The linear variation of k_{obs} with [CO] that was observed for $W(CO)_3(PPh_3)_2Br_2$ shows that this process has a first-order dependence of [CO] on the rate. This rate law is therefore first order in both transient and CO as is the reaction of $M(CO)_2(DCE)(PR_3)_2X_2$ with CO. Since the loss of two ligands in one flash pulse has not been observed in fluid solution[26] and the reaction of the dicarbonyl with CO has been accounted for, something other than CO loss must be occurring.

Infrared spectroscopy indicates that phosphine loss accounts for the photoprocess observed. When a solution containing equimolar concentrations of $Mo(CO)_3(PPh_3)_2Br_2$ and $W(CO)_3(PEt_3)_2Br_2$ in an IR cell is photolyzed by using a camera flash as a photolysis source, the spectrum shows a net change. If phosphine scrambling is occurring, there are potentially six products (eq 4). On the basis of the greater basicity of PEt_3 and

$$Mo(CO)_3(PPh_3)_2Br_2 + W(CO)_3(PEt_3)_2Br_2 \xrightarrow{h\nu} Mo(CO)_3(PPh_3)_2Br_2 + Mo(CO)_3(PEt_3)_2Br_2 + Mo(CO)_3(PPh_3)(PEt_3)Br_2 + W(CO)_3(PEt_3)_2Br_2 + W(CO)_3(PPh_3)_2Br_2 + W(CO)_3(PPh_3)(PEt_3)_2Br_2 \quad (4)$$

higher ν(CO) stretches for molybdenum carbonyl derivatives, it was expected that the four new compounds would have ν(CO) IR stretches intermediate in energy relative to the initial stretches. It was observed (Figure 2) that, following 70 flashes, bands at higher energy had shifted to slightly lower energy and bands at lower energy had shifted to slightly higher energy. Furthermore, there was significant band broadening and a general decrease in intensity, indicative of several compounds with bands that overlap imperfectly. As a test of this hypothesis, spectra were taken of $Mo(CO)_3(PPh_3)_2Br_2$, $W(CO)_3(PPh_3)_2Br_2$, $Mo(CO)_3(PEt_3)_2Br_2$, and $W(CO)_3(PEt_3)_2Br_2$. When digitally added, a close match of the actual final spectrum was obtained (see supplemental data). Secondary photochemistry was ruled out as a cause of the spectral changes because the difference spectrum after one flash is identical (although the peak intensities are smaller) to the final spectrum after 70 flashes.

It must be stressed that the only way that the phosphines can be scrambling is through phosphine loss following photon absorption. Formation of a dinuclear intermediate following CO loss that then scrambles phosphines is ruled out since PPh_3 is too large to permit dimerization of the dicarbonyl.[27] Halide photodissociation is dismissed as a possible explanation since the identity of the compound will not be changed on halide loss in the IR experiment. Also, Tyler et al. observed that the quantum yield for halide dissociation in metal halide carbonyl compounds is generally very small compared to the quantum yield for CO dissociation.[28] Conversely, significant phosphine photodissociation has been observed earlier in metal carbonyl compounds such as $Mo(CO)_4(PPh_3)_2$.[29] For example, the quantum yield for phosphine photodissociation in $Mo(CO)_4(PPh_3)_2$ is larger than that for carbon monoxide dissociation. A final piece of evidence is that a phosphine in $Mo(CO)_3(PPh_3)_2Cl_2$ could be thermally replaced by pyridine demonstrating that phosphine substitution is possible.[30]

The mechanism we propose to account for the observed photochemical behavior is shown in Scheme III. Absorption of a photon induces loss of phosphine ligand (eq 5). The phosphine deficient transient adds CO, forming $M(CO)_4(PR_3)Br_2$, a quasistable 18-electron intermediate (eq 6). CO addition is observed instead of recombination with PR_3 (eq 7), because CO is present in much greater concentrations under the experimental conditions. Hence $k_2[CO] \gg k_3[PR_3]$. The tetracarbonyl then reforms the tricarbonyl by slow attack of the free phosphine (eq 8), accounting for the photochromic behavior of the systems. In support of this mechanism, Vahrenkamp has reported the synthesis of $W(CO)_4LX_2$ as yellow solids, where L is an electron-rich ligand such as PMe_3 or $AsMe_3$ and X is a halide.[31] These are derivatives of the proposed intermediates formed by CO addition (eq 6). The triaryl congeners were not prepared presumably because they are not stable due to the less basic triarylphosphines. Especially pertinent is their observation that $W(CO)_4LBr_2$ readily loses CO and dimerizes. Thus, in our experiments, reaction of the tetracarbonyl with free phosphine (eq 8) to regenerate the starting material should be facile. The dimerization is inhibited by the free phosphine and excess CO present. The substitution of phosphine for CO would not be observable, however, because the proposed 18-electron tetracarbonyl intermediate would not be expected to show low-energy visible bands and high-energy absorbances would be masked by unreacted starting material.[32]

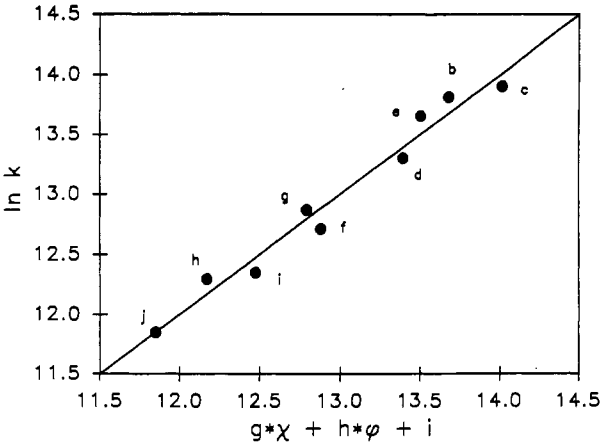

Figure 4. Relationship obtained by multiple linear regression for the reaction of $M(CO)_3(PR_3)(DCE)Br_2$ with CO with the equation in $k_{expt} = g\chi + h\phi + i$. A correlation coefficient of 0.976 was obtained between the observed and calculated values of ln k_{expt}. Refer to Table V for lettering system.

Scheme III

$$M(CO)_3(PR_3)_2Br_2 \xrightarrow{h\nu} M(CO)_3(PR_3)(DCE)Br_2 + PR_3 \quad (5)$$

$$M(CO)_3(PR_3)(DCE)Br_2 + CO \rightarrow M(CO)_4(PR_3)Br_2 + DCE \quad (6)$$

$$M(CO)_3(PR_3)(DCE)Br_2 + PR_3 \rightarrow M(CO)_3(PR_3)_2Br_2 + DCE \quad (7)$$

$$M(CO)_4(PR_3)Br_2 + PR_3 \rightarrow M(CO)_3(PR_3)_2Br_2 + CO \quad (8)$$

Substituent Effects on the Rate. The fastest reactions of phosphine-deficient transients with CO are observed for the derivatives containing strongly electron-withdrawing phosphines such as $P(C_6H_4$-*p*-$Cl)_3$, while the slowest rates are observed for $P(C_6H_4$-*p*-$OMe)_3$ derivatives. This is consistent with electron donation to the electron-poor intermediate lessening the electron deficiency at the metal center and decreasing its Lewis acidity. The metal also clearly has an effect on the rate of reaction. Tungsten derivatives react more sluggishly than the corresponding molybdenum derivatives. This is a typical result in the substitution reactions of group 6 carbonyls[33] and was also observed in the

(26) Seder, T. A.; Church, S. P.; Weitz, E. *J. Am. Chem. Soc.* **1986**, *108*, 4721.
(27) (a) Brisdon, B. J.; Hodson, A. G. W. *Inorg. Chim. Acta* **1987**, *128*, 51. (b) Normally dimerization of the dicarbonyl is not observed for the PEt_3 derivative. $[W(CO)_2(PEt_3)_2Cl_2]_2$ has been prepared, however, by treatment of $W(CO)_2(PEt_3)_2$(trop)Cl (trop = tropolonate) with $AlCl_3$. (c) Brower, D. C.; Winston, P. B.; Tonker, T. L.; Templeton, J. L. *Inorg. Chem.* **1986**, *25*, 2883.
(28) Pan, X.; Philbin, C. E.; Castellani, M. P.; Tyler, D. R. *Inorg. Chem.* **1988**, *27*, 671.
(29) Darensbourg, D. J.; Murphy, M. A. *J. Am. Chem. Soc.* **1978**, *100*, 463.
(30) Unfortunately flash photolysis studies of tricarbonyl compounds in the presence of free phosphine was unsuccessful because net reaction, including CO substitution, occurred thermally.
(31) Umland, P.; Vahrenkamp, H. *Chem. Ber.* **1982**, *115*, 3555.
(32) Typically, 2–10% of the tricarbonyl is converted to dicarbonyl by the flash. The extinction coefficient of $M(CO)_4(PR_3)Br_2$ is not known, but if it is assumed that these are ligand field transitions as expected, similar amounts are converted to the phosphine loss transient leaving over half of the sample unchanged.
(33) Wilkinson, G.; Stone, F. G. A.; Abel, E. W. *Comprehensive Organometallic Chemistry*; Pergamon Press: New York, 1982; Vol. 3.

reaction of $M(CO)_2(DCE)(PR_3)_2Br_2$ with CO. It was not possible to test for solvation of the intermediate because of solubility limitations, however it is presumed that the intermediate is solvated. The sluggishness of the tungsten derivatives could then be rationalized as arising from a stronger interaction of the LUMO with a solvent DCE molecule producing a slower reaction with CO.

The free energy relationship of phosphine basicity (χ) and metal effect (ϕ) on the rate constant was examined. Figure 4 shows the plot of $\ln k_{expt}$ vs $g\chi + h\phi + i$ obtained by multiple linear regression. The values for coefficients g and h were 0.28 and 0.13 and the ratio g/h was 2.1. The linearity of the plot suggests the commonality of the reaction mechanism for the derivatives studied. The signs of the coefficients reinforce the previous inference that an electron-donating phosphine at a tungsten metal center inhibits the rate of reaction.

Comparison to the Reaction of $M(CO)_2(DCE)(PR_3)_2Br_2$ with CO. The rate constant for recombination of $M(CO)_3(DCE)(PR_3)Br_2$ with CO is generally 100 times larger than the value for the recombination of the corresponding $M(CO)_2(DCE)(PR_3)_2Br_2$ derivative with CO. Enhancement of the reactivity of the phosphine-deficient tricarbonyl derives from the fact that it has one less phosphine and one more carbonyl than $M(CO)_2(DCE)(PR_3)_2Br_2$. It therefore has less steric bulk to impede an incoming carbon monoxide and less electron density at the metal center. Both would magnify the reactivity of the electron-poor metal center toward CO.

No fast process was observed for the PEt_3 derivatives. Indirect evidence that it occurs for $W(CO)_3(PEt_3)(DCE)Br_2$ is evidenced in the observation that phosphine scrambling was invoked to explain the infrared spectra of $Mo(CO)_3(PPh_3)_2Br_2$ and $W(CO)_3(PEt_3)_2Br_2$ after photolysis. Apparently the transient collapses within the lifetime of the lamp flash and can not be directly observed.

Summary

Flash photolysis of $M(CO)_3(PR_3)_2X_2$ was shown to undergo two independent photoprocesses: CO loss and PR_3 loss. The CO loss products react directly with CO. The intimate mechanism of CO addition for $M(CO)_2(DCE)(PR_3)_2X_2$ depends on the steric bulk of the phosphine. Derivatives with large phosphine ligands appear to react by a single-step CO addition to the solvated dicarbonyl, while derivatives with smaller phosphines require a two-step reaction. The steric bulk of the phosphine affects the rate in a discontinuous fashion. At small phosphine cone angles ($\leq 137°$) there is no effect of cone angle on the rate. Phosphines with larger cone angles show an inhibitory effect on the rate which increases with increasing phosphine steric bulk. The phosphine loss transient, only observed for bromide triarylphosphine derivatives, was analyzed for electronic effects through linear free energy relationships. Its back-reaction with CO was 100-fold faster than for the CO loss transient because of the more open, more electron-poor nature of the transient. The process was photochromic, implying that phosphine freed by photon absorption replaces a CO in the intermediate product reforming the tricarbonyl.

Acknowledgment. We are grateful to Prof. Mauri Ditzler for allowing access to diffuse relfectance instrumentation and to Prof. Warren Giering for helpful discussions on phosphine steric effects. We acknowledge a William and Flora Hewlett Foundation Grant from the Research Corp. and thank the donors of the Petroleum Research Fund, administered by the American Chemical Society, and the National Science Foundation through Grant No. CHE87-12543 for support of this research. R.M.J. acknowledges the National Science Foundation (USE-8852774) for support of the Holy Cross NMR facilities. J.L.H. acknowledges a Vermont EPSCoR-NSF grant for purchase of the X-ray diffractometer (Grant No. R11-8610679) and Dr. C. Campana for helpful discussions.

Supplementary Material Available: Plots of the fast and slow decay traces for both $Mo(CO)_3(PPh_3)_2Br_2$ and $W(CO)_3(PPh_3)_2Br_2$, the plot of observed rate constant vs [CO] for reaction $W(CO)_2(PEt_3)_2Br_2$ and $W(CO)_3(PPh_3)Br_2$ with CO, a linear free energy plot for the reaction of $M(CO)_2(DCE)(PEt_3)Br_2$ with CO, a plot showing a comparison of experimental and predicted spectra for the solution produced by photolysis of $Mo(CO)_3(PPh_3)_2Br_2$ and $W(CO)_3(PEt_3)_2Br_2$, and tables of the atomic coordinates and equivalent isotropic displacement coefficients, the anisotropic displacement coefficients, and hydrogen atom parameters (9 pages); a listing of the observed and calculated structure factors (7 pages). Ordering information is given on any current masthead page.

Contribution from the Department of Chemistry,
Simon Fraser University, Burnaby, BC, Canada V5A 1S6

Formation and Decomposition of Peroxovanadium(V) Complexes in Aqueous Solution

Jaswinder S. Jaswal and Alan S. Tracey*

Received March 13, 1991

^{51}V NMR spectroscopy has been used to characterize the complexes formed between hydrogen peroxide and vanadate under near-neutral conditions in aqueous solution. The formation constants of the mono-, di-, and triperoxovanadates and tetraperoxodivanadate have been measured and the proton requirements for product formation determined. Under the conditions of these studies, the peroxide was found to undergo slow catalytic decomposition. Studies of the decomposition reaction suggested that the monoperoxovanadate is involved in a disproportionation of the hydrogen peroxide, which occurs by a combination of photo- and thermochemical mechanisms. The decomposition reaction is strongly inhibited by the presence of peptides.

Introduction

The interactions that occur between hydrogen peroxide and vanadium oxoanions have been of interest for many years. The studies of these systems are attracting increasing interest in biochemistry because it is becoming increasingly clear that peroxovanadium compounds can have potent biochemical effects.

Over the past 4 years, an insulin mimetic behavior of vanadate in solution with hydrogen peroxide has been well established.[1-4] The insulin-like synergistic effects of hydrogen peroxide with vanadate exceed those seen with vanadate or hydrogen peroxide alone, suggesting strongly that peroxovanadates are responsible for the effects observed. Other work has shown that peroxovanadates have antitumor activity in mice,[5] and efforts are being

(1) Heffetz, D.; Bushkin, I.; Dror, R.; Zick, Y. *J. Biol. Chem.* **1990**, *265*, 2896-2902.

(2) Fantus, I. G.; Kadota, S.; Deragon, G.; Foster, B.; Posner, B. I. *Biochemistry* **1989**, *28*, 8864-8871.

(3) Kadota, S.; Fantus, I. G.; Deragon, G.; Guyda, H. J.; Hersh, B.; Posner, B. I. *Biochim. Biophys. Res. Commun.* **1987**, *147*, 259-266.

(4) Kadota, S.; Fantus, I. G.; Deragon, G.; Guyda, H. J.; Posner, B. I. *J. Biol. Chem.* **1987**, *262*, 8252-8256.

0020-1669/91/1330-3718$02.50/0